

The lives of FR I radio galaxies

P. Parma ^{a,1}, M. Murgia ^{b,2}, H.R de Ruiter ^{c,3}, R. Fanti ^{d,4}

^a*Istituto di Radioastronomia, via Gobetti 101, I-40129 Bologna, Italy*

^b*Istituto di Radioastronomia, via Gobetti 101, I-40129 Bologna, Italy and Dipartimento di Astronomia, Universita' di Bologna, via Ranzani 1, I-40127, Italy*

^c*Istituto di Radioastronomia, via Gobetti 101, I-40129 Bologna, Italy and Osservatorio Astronomico, via Ranzani 1, I-40127, Italy*

^d*Istituto di Radioastronomia, via Gobetti 101, I-40129 Bologna, Italy and Dipartimento di Fisica, Universita' di Bologna, via Irnerio 46, I-40126, Italy*

Abstract

After a brief introduction to the morphological properties of FRI radio sources, we discuss the possibility that FRI jets are relativistic at their bases and decelerate quickly to non-relativistic velocities.

From two-frequency data we determine spectral index distributions and consequently the ages of FRI sources. We show that in the large majority of cases synchrotron theory provides unambiguous and plausible answers; in a few objects re-acceleration of electrons may be needed. The derived ages are of the order $10^7 - 10^8$ years, $\sim 2 - 4$ times larger than the ages inferred from dynamical arguments and a factor $\sim 5 - 10$ larger than the ages of FR II sources. The linear sizes of FRI and FR II sources make it unlikely that many FR II's evolve into FRI's.

A brief discussion is given of the possibility that radio sources go through different cycles of activity.

1 FR I radio sources: morphologies and jet velocities

Low and high luminosity radio sources appear to be very different, in fact so much so, that the Fanaroff and Riley classification not only stresses the morphological differences but also suggests fundamental physical differences.

¹ E-mail: parma@astbo1.bo.cnr.it

² E-mail: murgia@astbo1.bo.cnr.it

³ E-mail: deruiter@kennet.bo.astro.it

⁴ E-mail: rfanti@astbo1.bo.cnr.it

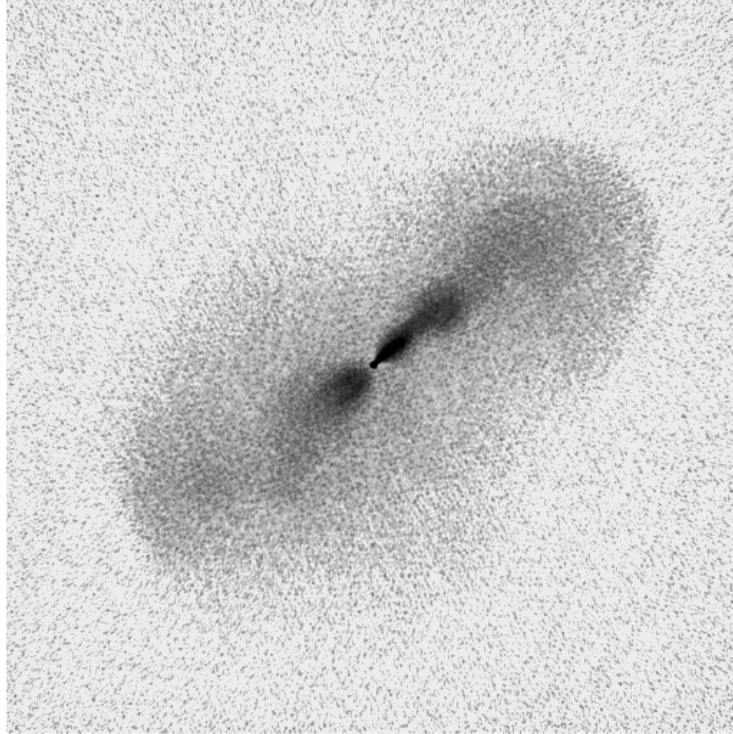


Fig. 1. B2 0206+35, a typical FRI source.

FRI sources are much more common in the universe than FRIIs and show much more diversity. While FRIIs are quite homogeneous in morphology the FRI class is a kind of “mixed bag” where one finds very different sources, which have, apart from the similar radio power, only one feature in common: hot-spots at the outer end of the lobes are never seen. 3C31 with its twin jet ending in characteristic plumes has often been cited as a kind of prototype FRI source, but in reality double lobed sources with jets are the rule (Fig. 1): In the B2 sample of low luminosity radio galaxies 3% are of the 3C 31 type, 50 % are double lobed with (single or double) jets and the rest is a mixture of tailed sources (NATs and WATs) and naked jets.

Naked jets (see e.g. Fig. 2) occur preferably at the low end of the power range covered by the B2 sample ($< 10^{23} \text{W Hz}^{-1}$), while at the upper end ($\sim 10^{25} \text{W Hz}^{-1}$) we find sources with an overall FR I structure but with one-sided jets and hot spots in the middle of the lobes (Fig. 3).

A characteristic feature of FR I sources is the presence of prominent twin jets that are usually very symmetrical at large scales; however the jets tend to be very asymmetric close to the nucleus, at the jet base. This asymmetry is more pronounced in the stronger sources: the jets tend to become one-sided, more collimated, while brightness knots appear as we go to higher powers.

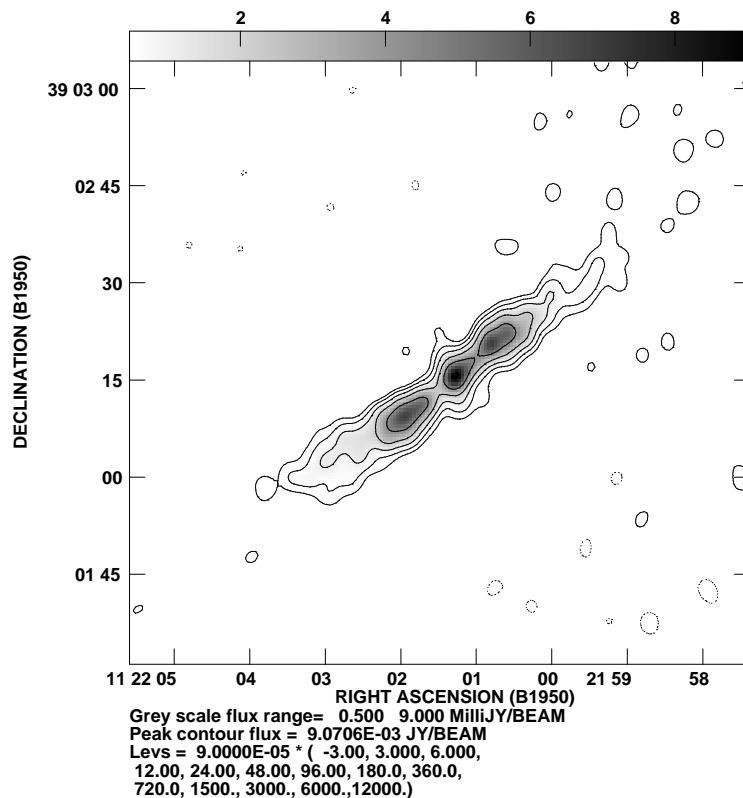


Fig. 2. B2 1122+39, a “naked” jet source.

A recent study done by Laing et al. (1999), of the side-to-side asymmetries on kiloparsec scales in the jets of FRI radio galaxies selected from the B2 sample, shows that differences between the jets at a given distance from the nucleus can be interpreted as effects of Doppler beaming on intrinsically symmetrical flows. The observed asymmetries are consistent with the hypothesis that the jet velocities close to the core are (mildly) relativistic, and that they decelerate further out. The length of the deceleration region depends on total power of the source, and ranges from ~ 2 kpc for $P < 10^{24}$ WHz^{-1} to ~ 10 kpc for the stronger sources. This point is illustrated in Fig. 4 which shows the jet to counter-jet brightness ratio as function of normalized core power P_{cn} at different locations from the core. P_{cn} is an independent orientation indicator which we expect to correlate with the brightness ratio where the flow is relativistic. This is indeed the case for the ratio at the flaring point for both powerful and weak sources (fig. 4a). At 2 kpc from the core the correlation still exists for powerful sources (fig. 4 b) but at 10 kpc the correlation has disappeared in both categories of sources (fig. 4c).

Also the residual velocity, after the deceleration has taken place, depends on total power. The jet velocity can be derived by estimating the energy flux through the jet, F_E , from the corresponding lobe luminosity (Bicknell 1986,

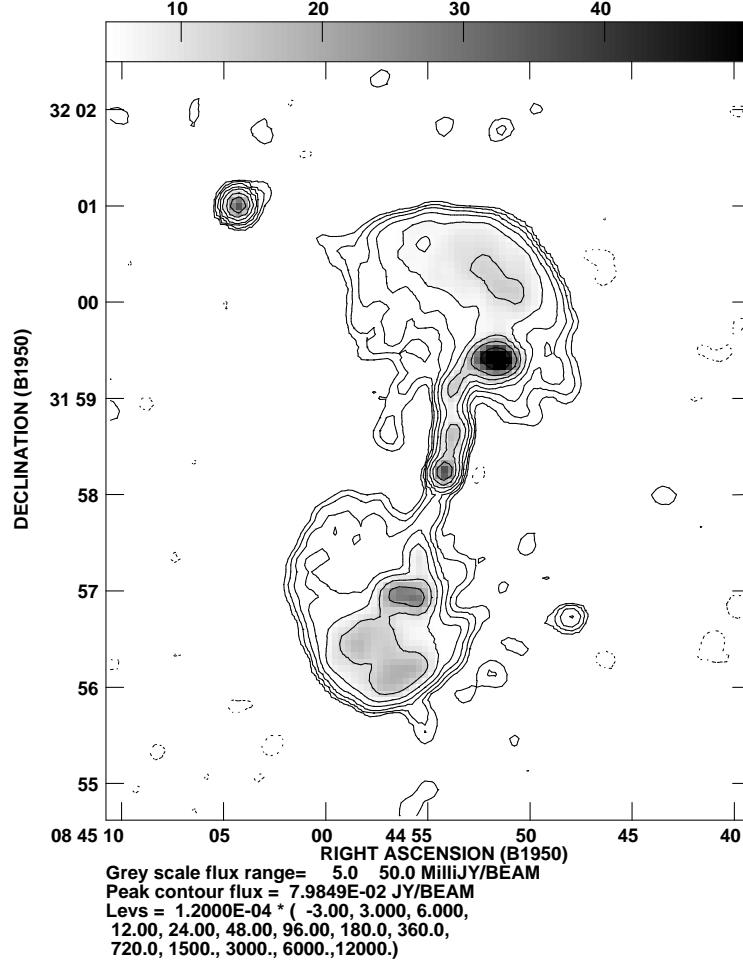


Fig. 3. B2 0844+31, a FRI - FRII source.

1994). The resulting velocity estimates, v_{eb} , are plotted against total power in Fig. 5. The median v_{eb} increases with P_t , from $\sim 10^3 \text{ km s}^{-1}$ ($\beta = 0.03$) at $P_t = 10^{22} \text{ WHz}^{-1}$ to $\sim 3 \times 10^4 \text{ km s}^{-1}$ ($\beta = 0.1$) at $P_t = 10^{25} \text{ WHz}^{-1}$ and the corresponding energy fluxes are in the range $10^{33} - 3 \times 10^{36} \text{ W}$. The median relation between v_{eb} and P_t is in agreement with estimates from jet asymmetry in that Doppler beaming is predicted to be significant at 10 kpc only for the most powerful sources.

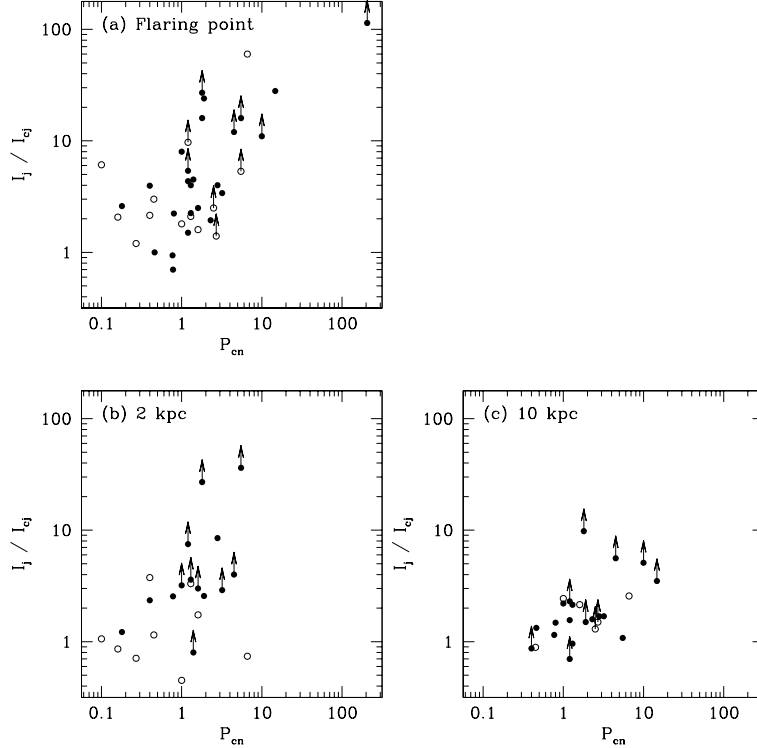


Fig. 4. Plots of brightness ratio against normalized core power. Open circles: $P_t < 10^{24} \text{ WHz}^{-1}$; filled circles: $P_t \geq 10^{24} \text{ WHz}^{-1}$. (a) Flaring point, (b) 2 kpc from core, (c) 10 kpc from core.

2 The ages of FR I radio sources

2.1 Introduction

The determination of ages of extragalactic radio sources is one of the key points for any theoretical model that wants to explain the origin and evolution of radio galaxies.

One of the methods for determining source ages is the study of the radio spectra, for which synchrotron theory predicts a frequency break due to the radiative energy losses, which drifts in time. According to various source evolution models, relativistic electrons in different regions of the source are deposited there at different times, so that the break frequency effectively is a clock that indicates the time elapsed since their production.

For a limited number of objects, detailed studies of the radio spectra across the emitting regions have produced break frequency and source age maps (see e.g. Alexander 1987; Carilli et al. 1991; Feretti et al. 1998). However, in the majority of these studies the radio spectra across a source are based on only one pair of frequencies, so that the break frequency cannot be seen directly

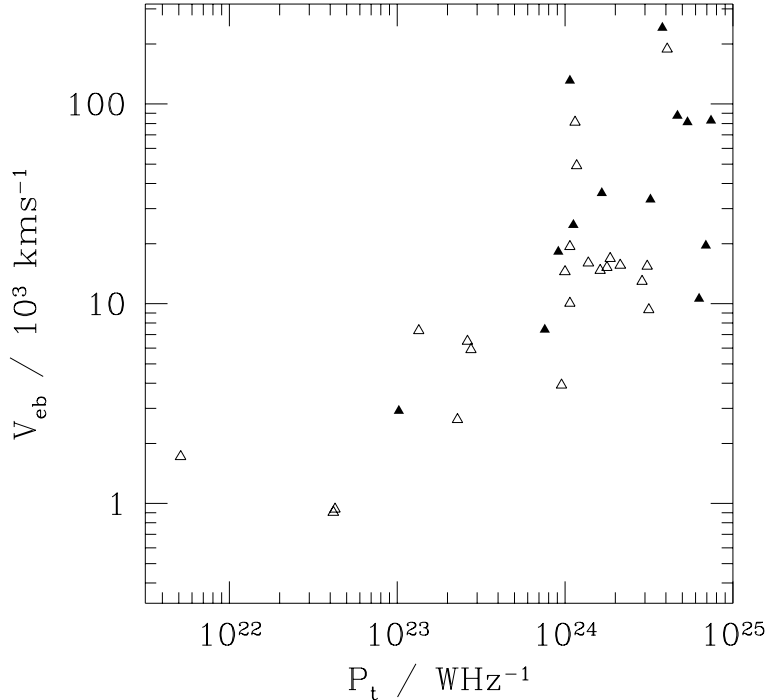


Fig. 5. A plot of the velocity at 10 kpc estimated from energy balance against power. Filled triangles: sources which have $I_j/I_{cj} > 1.5$ at 10 kpc from the nucleus (or the end of the jet, if closer). Open triangles: sources with $I_j/I_{cj} \leq 1.5$.

from the data. Nevertheless, with some additional assumptions which find their justification from the results obtained from the well studied objects, the break frequency can be estimated with reasonable accuracy. In fact, the data available in the literature which concern a large number of powerful 3C sources are analyzed in this way (see e.g. Alexander & Leahy 1987; Leahy et al. 1989; Liu et al. 1992).

Recently a two frequency spectral study has been done of a representative subsample of B2 radio galaxies (Parma et al., 1999); in which the radiative ageing of the relativistic electrons caused by synchrotron and inverse Compton (I.C.) energy losses is discussed. This study is complementary to those dealing with powerful 3CR radio sources: the B2 radio sources are less powerful by about two orders of magnitude (we use $H_0 = 100 \text{ km s}^{-1} \text{ Mpc}^{-1}$).

2.2 The data

The B2 sample of radio sources, which contains about a hundred objects, was obtained from identification of B2 radio sources with bright elliptical galaxies (see Colla et al. 1975; Fanti et al. 1978). Because of the selection criteria, the sample is dominated by radio galaxies with a power typically between 10^{23} and 10^{25} WHz^{-1} at 1.4 GHz. Most are FRI sources.

The sample has been extensively studied with different VLA configurations at 1.4 GHz (see references in Fanti et al. 1987) and more recently at 5 GHz Morganti et al. (1997).

From the original B2 sample only sources with a ratio of overall source size to beam size ≥ 10 were selected, for a total of 32 sources. For each source the average of the two frequency spectral index $\alpha_{5.0}^{1.4}$ was computed in slices perpendicular to the source axis in order to study the variation of the spectral index along the source major axis. Only data with a signal to noise ratio > 5 were used. The slices are one beam across, so that the data points are practically independent. Regions containing radio jets and hot spots were excluded. Spectral index errors along the profiles are mostly determined by the map noise and in a minority of cases by dynamic range. They are typically ~ 0.05 , but can be as high as ≥ 0.1 in the faintest regions considered. Unfortunately the cut-off imposed on brightness at 5 GHz introduces a bias against the inclusion of regions with very steep spectra.

From a literature search additional information on the spectral index distribution were recovered of 15 more objects in the B2 radio galaxy sample. These data have been re-analyzed in order to ensure as much as possible homogeneity.

In most objects the spectral index clearly varies with distance from the core. The spectrum either steepens from the lobe outer edge inward (hereafter referred as “spectral type 2”), or from the core outward (“spectral type 1”). Only a minority of sources do not show any significant spectral index trend. In Fig. 6 we show the behaviour of the spectral index for type 1 and type 2 sources separately. This double behaviour had already been pointed out some time ago by Jägers (1981). In the “spectral type 2” sources the older electrons are found closer to the core. This class contains essentially sources with double lobed morphology, of both FR I and FR II type. Their spectral behaviour is that expected on the basis of standard source models where the radiating particles are deposited at different times at the end of an advancing beam and remain in that position or flow back at some speed toward the core. In this model the closer to the core the older they are.

In the “spectral type 1” the spectral index steepens away from the core. This class is known to contain “3C 31 like” objects, WATs, and NATs (see, e.g., Jägers, 1981). These are the type of objects for which (Katz-Stone & Rudnick 1997) have found two distinct components, a flat spectrum jet surrounded by a steeper spectrum sheath

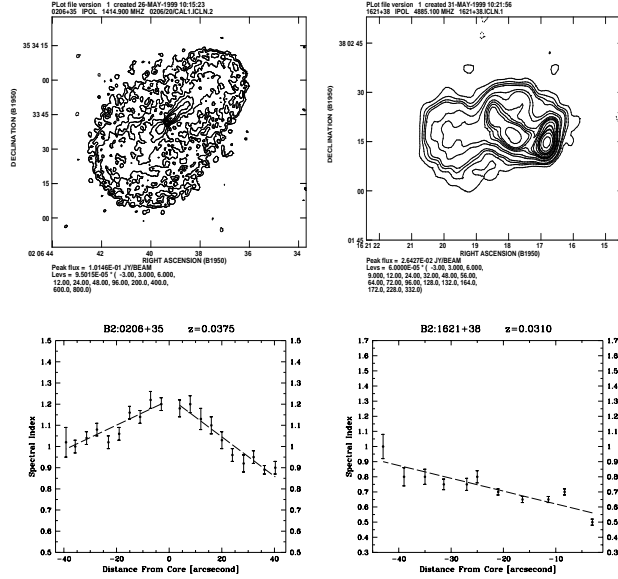


Fig. 6. Left: spectral type 2; right: spectral type 1

2.3 The models and the assumptions

The spectral trends along the sources are interpreted in terms of radiative ageing of the relativistic electrons by synchrotron and I.C. processes.

Theoretical synchrotron-loss spectra have been computed numerically (Murgia 1996) from the synchrotron formulae (e.g., Pacholczyk 1970). It is assumed that the synchrotron and I.C. losses dominate and that expansion losses and re-acceleration processes can be neglected

Two models are generally considered: i) the Jaffe-Perola (JP) model (Jaffe & Perola 1974), in which the time scale for continuous isotropization of the electrons is assumed to be much shorter than the radiative time-scale; ii) the Kardashev-Pacholczyk (KP) model (Kardashev 1962) in which each electron

maintains its original pitch angle. The JP model has been used since the I.C. energy losses due to the microwave background radiation are as important as the synchrotron losses, and in the former random orientations are expected between electrons and photons.

The two frequency spectral index $\alpha_{\nu_2}^{\nu_1}$ allows the computation of the break frequency, ν_{br} , in various regions of the source, using the synchrotron-loss spectrum for the JP model. The break frequency is used to determine a spectral age, based on the formula:

$$t_s = 1.61 \times 10^3 \frac{B^{0.5}}{(B^2 + B_{CMB}^2)(\nu_{br}(1+z))^{0.5}}$$

where the synchrotron age t_s is in Myrs, the magnetic field B is in μG , the break frequency ν_{br} in GHz and $B_{CMB} = 3.2 \times (1+z)^2 \mu G$ is the equivalent magnetic field of the cosmic microwave background radiation. It is assumed that the magnetic field strength is uniform across the source and has remained constant over the source life. The magnetic field is computed using the “minimum energy assumption”. Equality of protons and electrons energy was assumed, a filling factor of unity, a radio spectrum ranging from 10 MHz to 100 GHz and an ellipsoidal geometry. For most of the objects of the sample the computed magnetic field is within a factor 2 of B_{CMB} . This ensures that the synchrotron ages t_s are relatively independent of moderate deviations from the minimum energy conditions.

Fig. 7 shows how the radiative life time depends on the ratio B/B_{eq} . For $0.5 < B_{eq}/B_{CMB} < 2$, deviations from equipartition have a small effect on the computed lifetime if $B \leq 2 \cdot B_{eq}$.

2.4 Spectral analysis

For the majority of the sources the quality of spectral information is comparable in the two lobes, and the spectral trends are rather similar when the errors are taken into account. Therefore the two lobes were analyzed together, instead of considering them separately. This was done by folding the spectral profiles of the two lobes onto each other, after having normalized the coordinates along the lobe axis to the maximum lobe extent (Fig. 8).

The folded spectral index plots along the source axis were fitted with a relationship of the type:

$$\nu_{br} \propto x^{-2}$$

where x is the normalized distance from the outer lobe edge or from the core according to the observed steepening trend. The above law is expected on the basis of the relation between radiative age and break frequency, if x is proportional to time, i.e. assuming a constant expansion speed. From it a best

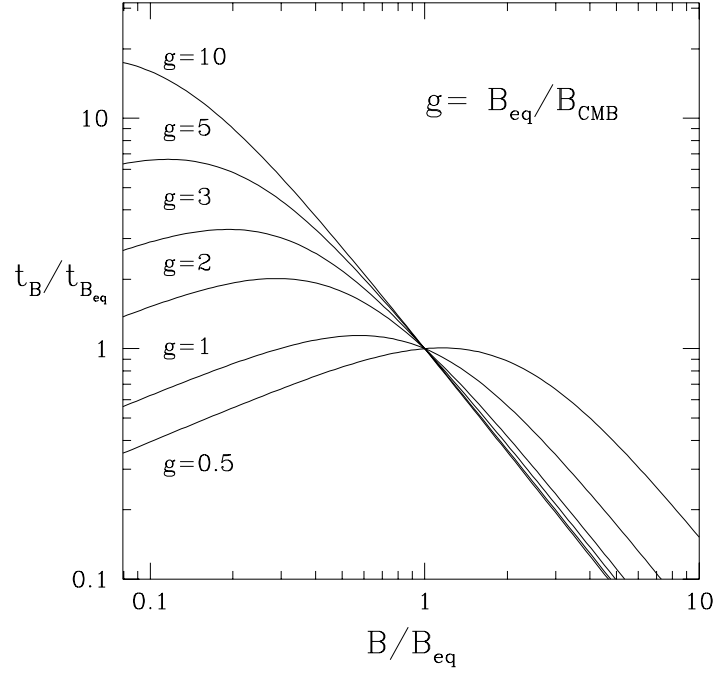


Fig. 7. The radiative lifetime as a function of the ratio B/B_{eq} .

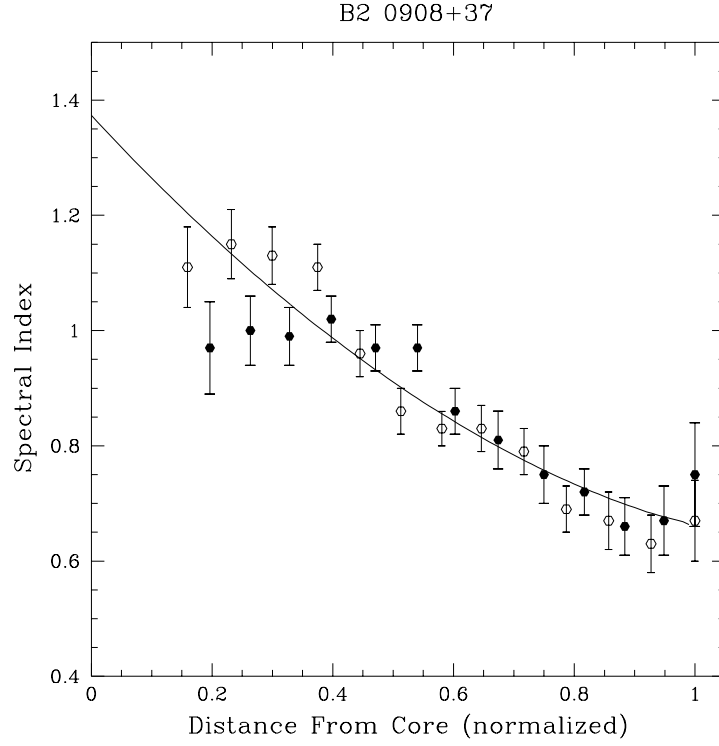


Fig. 8. The distances are normalized to the maximum extent of a lobe. The full line is the best fit of the radiative model.

estimate of α_o was obtained, i.e. the spectral index close to the outer edge of the lobe or close to the core, according to the observed spectral profile. This, with a few exceptions, is assumed to be equal to the injection spectral index, α_{inj} .

The mean value of α_o is ~ 0.65 , with a dispersion ~ 0.1 . In this way, from the folded spectral profiles, we derived the variation of the break frequency as a function of position, averaged over the two lobes. Extrapolating it to the inner or outer part of the source, it is possible to obtain the “minimum break frequency”, ν_{br-min} , namely the break frequency of the oldest electrons, that we use for determination of the source age. For the large majority of the sources the extrapolation introduces only minor additional uncertainties. The computed values of ν_{br-min} range from a few GHz up to several tens of GHz.

Considering the errors in the spectral index (≥ 0.05) and the uncertainty in α_{inj} (≤ 0.1), the uncertainty in ν_{br-min} can be quantified as:

$$\Delta\nu_{br}/\nu_{br} \leq 0.08 \cdot (\nu_{br}(GHz))^{0.5}.$$

This implies that only values of $\nu_{br-min} \leq 30$ GHz are significant, which is hardly surprising given that our highest frequency is a factor six lower. The errors on t_s , for a given magnetic field, are $\sim 15\%$, for break frequencies of a few GHz, increasing up to $\geq 40\%$ for break frequencies ~ 30 GHz. Had we used the KP model, t_s would be shorter by $\sim 10\%$.

The radiative lifetimes are in the range of $10^7 - 10^8$ years. The possibility of missing source areas with steeper spectra cannot be excluded. Therefore the t_s given are lower limits on the source ages.

The distributions of radiative ages, t_s , for the two spectral classes are very similar.

2.5 *Is there particle re-acceleration?*

The fits to the data in general are good, in the sense that they describe well the overall trend of $\alpha_{5,0}^{1.4}$ versus x .

There are however a few objects where the break frequency does not always seem to increase with x as expected from the simple synchrotron/I.C. model.

The saturation of $\alpha_{5,0}^{1.4}$ to a constant value would indicate that the break frequency, after an initial decrease, does not decrease anymore. A possible explanation of this is that a re-acceleration process is acting, which compensates in part for the radiative energy losses and causes a freezing of the break energy

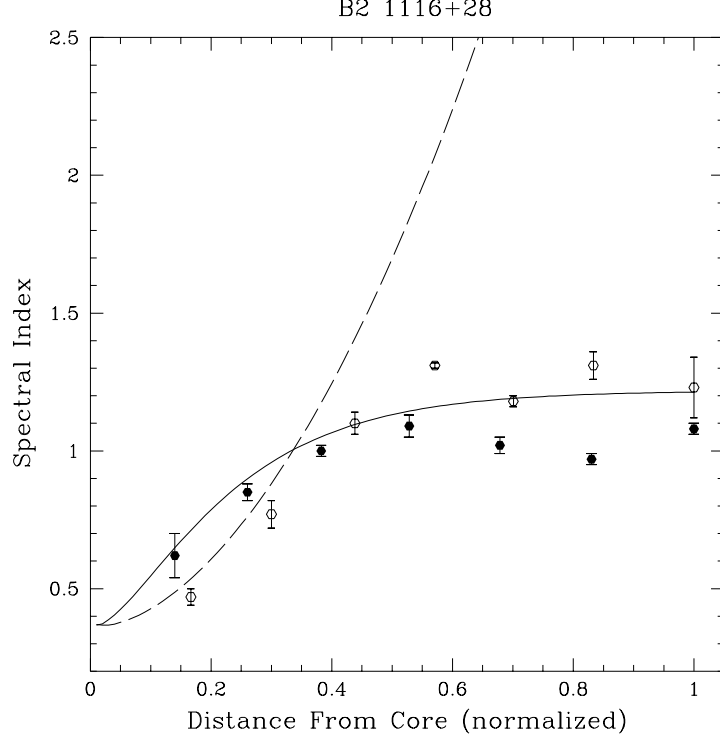


Fig. 9. Spectral index as a function of distance from the core. The full line represents the re-acceleration model

at that value where the radiative and the acceleration time scales are equal. Of course, if re-acceleration processes are working, the ages estimated would be underestimated. Expressing the re-acceleration process as:

$$dE/dt = E/\tau_a,$$

where E is the particle energy, and τ_a is the acceleration time scale, the break frequency, as a function of time (see Kardashev, 1962), is given by:

$$\nu_{br} \propto \frac{B}{(B^2 + B_{CMB}^2)^2} \frac{1}{(1 - e^{-t/\tau_a})^2 \tau_a^2} \propto \frac{\rho^2}{(1 - e^{-\rho x})^2},$$

where ρ is the ratio of the source age to the re-acceleration time scale τ_a and x is the normalized distance from the outer lobe edge or from the core according to the observed steepening trend.

The above law naturally leads to a saturation of ν_{br} when $t \geq \tau_a$.

We have re-fitted all the spectral profiles with the above formula and derived a value of ρ for each source and corresponding source age, t'_s , which is related to the previous one (t_s) by:

$$t'_s = \frac{t_s \rho}{1 - e^{-\rho}}$$

For at least 70% of the objects the results are not much different from the purely radiative model. For those we find $0 \leq \rho \leq 2$ (the median value is 1.1) and the lifetimes are modified by less than a factor 2. Time scales for re-acceleration must be typically $\geq 4 \cdot 10^7$ years.

However for a few sources (0844+31, 1116+28, 1521+28, 1528+29) the fit improves, while $\rho > 5$ suggests that re-acceleration may be present (Fig. 9).

Their ages should then be raised by factors from ~ 6 to ~ 10 with respect to the “radiation only” model. These objects are among those in which the spectrum steepens away from the core.

There are no significant negative values for ρ , which indicates either that expansion losses are negligible or that they are well compensated by re-acceleration processes.

2.6 Discussion

2.6.1 Spectral ages and source sizes

It has been investigated whether there is a relationship between radiative age and source size. Indeed a significant correlation is present as shown in Fig. 10. A linear fit between the logarithms of age and linear size gives:

$$LS \propto t_s^{0.97},$$

where the uncertainty in the exponent is 0.17.

One might think that the correlation between linear sizes and the radiative ages shown could be a partial consequence of the equipartition assumption. In fact, $B_{\text{eq}} \propto LS^{-6/7}$ implies that $LS \propto \tau_{\text{syn}}^{7/9}$. In our case the computed magnetic field is within a factor 2 of B_{CMB} , therefore the synchrotron ages are relatively independent from the minimum energy conditions.

The advance speed of the lobes, deduced from the synchrotron ages, are in the range of $0.5 - 5 \cdot 10^3$ km/sec. There is no difference between the two spectral classes.

2.6.2 A comparison between spectral and dynamical ages

The synchrotron ages, t_s , have been compared with the dynamical ages, t_d , evaluated from simple ram-pressure arguments. The expansion velocity of the lobes is given by the relation:

$$v_{\text{exp}} \sim \left[\frac{\Pi}{A} \frac{1}{m_p n_e} \right]^{0.5}$$

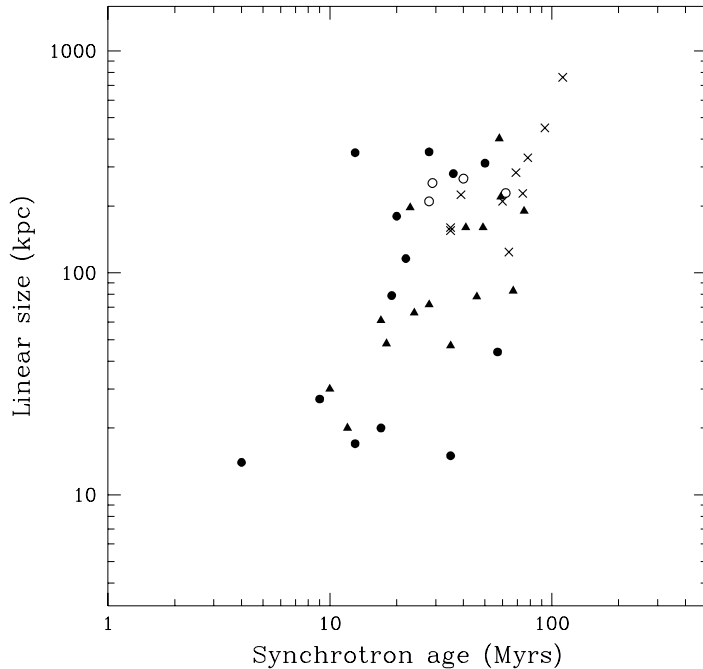


Fig. 10. Linear size as a function of spectral age of the source. The crosses represent the sources taken from the literature, the dots type 1 spectra, the open circles referring to four sources whose radiative lifetimes could be definitely longer. The triangles represent type 2 spectra.

where Π is the jet thrust and A is the size of the area over which it is discharged.

The most simplistic assumption is to identify the Π/A ratio with the hot spot pressure. The front surface minimum pressures of the lobes, $p_{eq,f}$, as been used as the appropriate quantity for Π/A (Williams, quoted by Carilli et al., 1991).

The values found are typically 4 times the average minimum lobe pressure.

It is assumed that the jet thrust is constant over the source life time and that the source grows in a self-similar way, such that $p_{eq,f} \propto R_{kpc}^{-2}$. Finally a run of the external density $n_e = n_o \times R_{kpc}^{-\beta}$ is assumed, with $n_o \sim 0.5 \text{ cm}^{-3}$ and $1.5 \leq \beta \leq 2$, according to Canizares et al. (1987). Under these assumptions there would be only a slight dependence, if any, of v_{exp} on source size, depending on the value of β .

The dynamical and radiative ages are correlated, but the dynamical ages in general are larger by a factor ~ 4 for $\beta = 1.5$ and ~ 2 for $\beta = 2$ (Fig. 11).

These discrepancies are believed to be not very serious for at least three reasons.

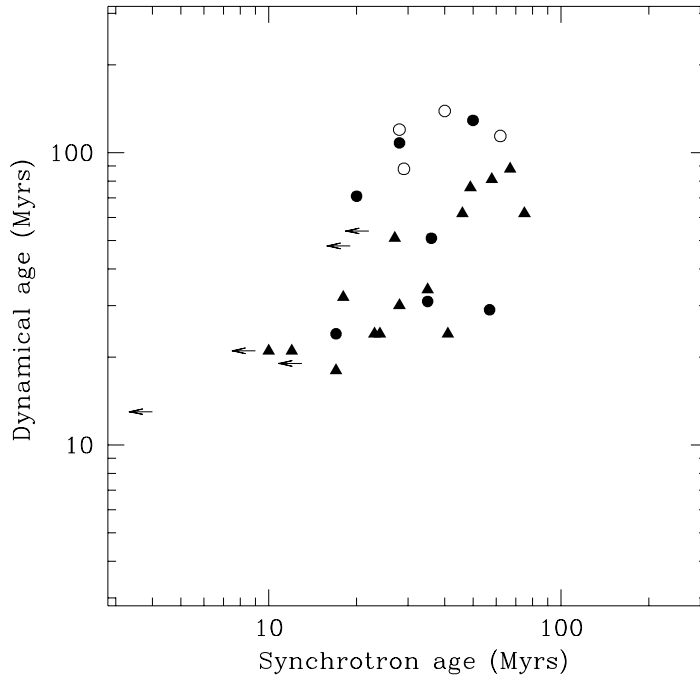


Fig. 11. Dynamical age vs spectral age of the source for $\beta = 2.0$. The dots represent sources with spectral type 1, the open circles referring to four sources whose radiative lifetimes could be definitely longer. Sources with spectra of type 2 are denoted by triangles. The arrows refer to sources for which the t_s are upper limits

First of all, the one-dimensional ram-pressure balance may not be realistic and discrepancies of a factor 2 or so are well possible, as mentioned above.

Second, the assumed central density may be a bit too high. A value around 0.1 cm^{-3} , which is not excluded by the X-ray data, would bring, for $\beta = 2$, the dynamical ages into closer agreement with the spectral ones.

Third, the ram-pressure dynamical ages depend on the minimum energy assumption. It has been shown that radio galaxies with luminosities like in the present sample usually have internal pressures larger than the minimum ones by a factor ≥ 5 (Morganti et al. 1988; Feretti et al. 1992). If the magnetic field is weaker than the one corresponding to minimum energy conditions by a factor ≥ 4 , the internal pressure increases by a factor ≥ 4 and the dynamical lifetime decreases by a factor ~ 2 . Anyway, the radiative lifetimes would change little. Likely both explanations may play a role in bringing t_s and t_d to a closer agreement.

Finally, the possibility of re-acceleration processes is another factor which goes in the direction of bringing the radiative and the dynamical timescales closer.

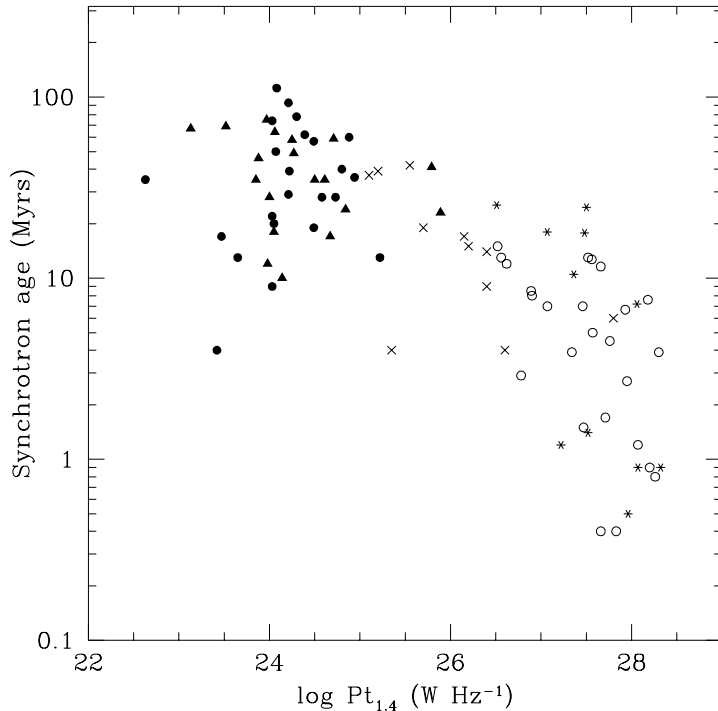


Fig. 12. Source age versus radio power at 1.4 GHz. The meaning of the symbols is as follows. Filled circles and triangles: B2 sources with type 1 and type 2 spectra, respectively; crosses: 3C galaxies with $z < 0.2$; open circles: 3C galaxies with $z > 0.2$; asterisks: 3C quasars.

2.6.3 Spectral ages and radio power: a comparison with the 3CR radio galaxies

The synchrotron ages derived for the B2 sample have been compared with the corresponding ones of 3CR sources as found by Alexander & Leahy (1987), Leahy et al. (1989) and Liu et al. (1992). When necessary the data were corrected, to take into account different assumed values for the Hubble constant.

It appears that the t_s of B2 sources are systematically larger than those of the 3CR sources by factors 5 - 10 (Fig. 12)

There are several possible reasons for these differences:

a) the radiative ages derived for the powerful sources (3CR) are heavily dependent on the equipartition magnetic field, B_{eq} , which is generally significantly larger than B_{CMB} . For $B \sim 1/4 \cdot B_{eq}$ the differences between the two sample would be greatly reduced.

b) Another possibility is that, if there is significant backflow in the powerful sources, there is mixing of the old and young electrons in the inner regions, which leads to a smoothing of the spectral break and an under-estimation of

the maximum radiative time scale.

Finally, the effect may be real, that is in low power sources like those of B2 sample, the nuclear activity lasts for a longer time. One could think of an evolutionary effect, in the sense that low power sources have evolved from high power sources and are therefore older. However, sources of B2 sample are on average smaller than powerful 3CR sources (de Ruiter et al., 1990) so that this explanation is unlikely in general, even if it cannot be excluded as an explanation in some individual cases.

Another possibility is a cosmological effect, since the 3CR sources are at much larger red-shifts than B2 radio galaxies.

3 Cycles of nuclear activity

The radiative ages thus computed are much smaller than the ages obtained from the radio luminosity function. A long time ago Schmidt (1966) found for powerful radio galaxies a harmonic-mean life time of about 10^9 years. This life time is the total time of the nuclear activity, not to be confused with the radiative loss age determined from spectral ageing arguments. The length of the active phase is related to the possible existence of duty cycles of nuclear activity. If the nuclear activity is not continuous, how often the interruptions occur and how long do they last? A duty cycle can be recognized as such if there is some mechanism that preserves the information of past nuclear activity for a long enough time to be recognized when a new cycle starts up. In the extended radio sources, such a mechanism is provided for by the radio lobes. If a new phase of activity should start before these “old” radio lobes have faded, and if this activity manifests itself by the production of jets, we can in principle recognize this as a new, young radio source embedded in a old relic structure. Of course this requires that the off time of the central activity is shorter than the fade-away time of the old radio lobes.

If the off time is long enough we have the double - double radio galaxies (DDRG) (Schoenmakers et al., 1999), radio sources with four lobes (Fig. 13). These radio sources have been discovered by Arno Schoenmakers in the WENSS survey and they consist of an inner double lobed radio structure as well as a larger outer double lobed structure. The inner and outer radio sources are well aligned, within 10 degrees. Following the definition of Schoenmakers, a DDRG consists of a pair of double radio sources with a common centre. The two lobes of the inner radio sources must have an extended, edge-brightened radio morphology. Up to now four DDRG have been found in WENSS survey, while three more can be found in the literature (3C445, 4C26.35 and 3C219). The DDRG have Mpc size (the outer components) and the power of the outer

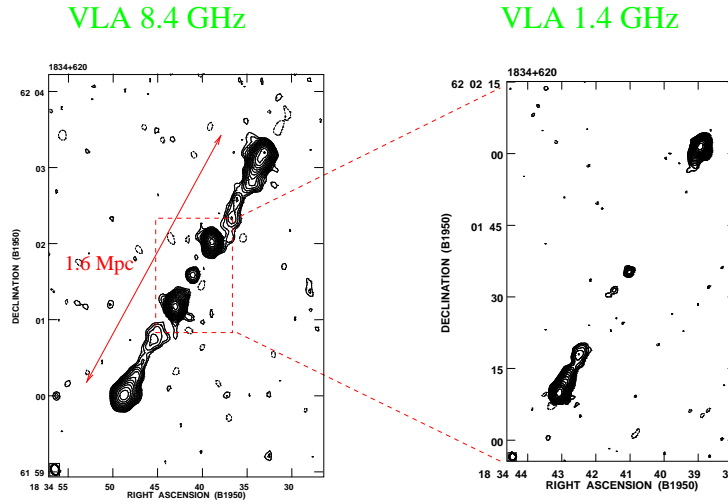


Fig. 13. The double-double radio galaxy WNB 1834+620. From Schoenmakers et al. 1999.

lobes is higher than the power of the inner lobes ($P_{1.4} \sim 10^{25} WHz^{-1}$).

The DDRG provide good evidence for recurrent radio activity in AGN: a large source is fading away while at the same time a smaller radio source emerges.

References

- Alexander P., 1987, MNRAS 225, 27
- Alexander P., Leahy J.P., 1987, MNRAS 225, 1
- Canizares C.R., Fabbiano G., Trinchieri G., 1987, ApJ 312, 503
- Carilli C.L., Perley R.A., Dreher J.W., Leahy J.P., 1991, ApJ 383, 554
- Colla G., Fanti C., Fanti R., Gioia I., Lari C., Lequeux J., Lucas R., Ulrich M.H., 1975, A&AS 20, 1
- de Ruiter H.R., Parma P., Fanti C., Fanti R., 1990, A&A 227, 351
- Fanti R., Gioia I., Lari C., Ulrich M.H. 1978, A&AS 34, 341
- Fanti C., Fanti R., de Ruiter H.R., Parma 1987, A&A 69, 57
- Feretti L., Perola G.C., Fanti R., 1992, A&A 265, 9
- Feretti L., Giovannini G., Klein U., Mack K.-H., Sijbring L.G., Zech G., 1998, A&A 331, 475
- Jaffe W.J., Perola G.C., 1974, A&A 26, 423

- Jägers W.J., 1981, Ph.D. Thesis, Leiden University
- Kardashev N.S., 1962, *Sov. Astron.* 6, 317
- Katz-Stone D.M., Rudnick L., 1997, *ApJ* 488, 146
- Laing R.A., Parma P., de Ruiter H.R., Fanti R., 1999, *MNRAS* 306, 513
- Leahy J.P., Muxlow T.W., Stephens P.W., 1989, *MNRAS* 239, 401
- Liu R., Pooley G.G., Riley J.M., 1992, *MNRAS* 257, 545
- Morganti R., Fanti R., Gioia I.M., Harris D.E., Parma P. & de Ruiter H., 1988, *A&A* 189, 11
- Morganti R., Parma P., Capetti A., Fanti R., de Ruiter H.R. and Prandoni I., 1997a, *A&AS* 126, 335
- Murgia M., 1996, Laurea thesis, Univ. of Bologna
- Pacholczyk A.G., 1970, *Radio astrophysics*, Freeman, San Francisco
- Parma P., Murgia M., Morganti R., Capetti A., de Ruiter H.R., Fanti R., 1999, *A&A* 344, 7
- Schmidt M., 1966, *ApJ* 146, 7
- Schoenmakers A.P., Rottgering H.J.A., de Bruyn A.G., van der Laan H., 1999, in: *The most distant galaxies*, eds. Rottgering H.J.A., Best P.N. & Lehnert M.D p. 497